

# Utrophin Binds Laterally along Actin Filaments and Can Couple Costameric Actin with Sarcolemma When Overexpressed in Dystrophin-deficient Muscle

Inna N. Rybakova,\* Jitandrakumar R. Patel,\* Kay E. Davies,†  
Peter D. Yurchenco,‡ and James M. Ervasti\*§

\*Department of Physiology, University of Wisconsin Medical School, Madison, Wisconsin 53706;

†Department of Human Anatomy and Genetics, University of Oxford, Oxford OX1 3QX, United Kingdom; and ‡Department of Pathology and Laboratory Medicine, Robert Wood Johnson Medical School, Piscataway, New Jersey 08854

Submitted September 11, 2001; Revised December 21, 2001; Accepted January 28, 2002  
Monitoring Editor: David Drubin

Dystrophin is widely thought to mechanically link the cortical cytoskeleton with the muscle sarcolemma. Although the dystrophin homolog utrophin can functionally compensate for dystrophin in mice, recent studies question whether utrophin can bind laterally along actin filaments and anchor filaments to the sarcolemma. Herein, we have expressed full-length recombinant utrophin and show that the purified protein is fully soluble with a native molecular weight and molecular dimensions indicative of monomers. We demonstrate that like dystrophin, utrophin can form an extensive lateral association with actin filaments and protect actin filaments from depolymerization *in vitro*. However, utrophin binds laterally along actin filaments through contribution of acidic spectrin-like repeats rather than the cluster of basic repeats used by dystrophin. We also show that the defective linkage between costameric actin filaments and the sarcolemma in dystrophin-deficient *mdx* muscle is rescued by overexpression of utrophin. Our results demonstrate that utrophin and dystrophin are functionally interchangeable actin binding proteins, but that the molecular epitopes important for filament binding differ between the two proteins. More generally, our results raise the possibility that spectrin-like repeats may enable some members of the plakin family of cytolinkers to laterally bind and stabilize actin filaments.

## INTRODUCTION

Costameres are assemblies of cytoskeletal and integral membrane proteins that physically connect the sarcolemmal membrane to the force-generating sarcomeric apparatus at the Z-line in striated muscle (Craig and Pardo, 1983; Pardo *et al.*, 1983). The dystrophin–glycoprotein complex is one element of costameres (Ervasti *et al.*, 1990; Ervasti and Campbell, 1991; Porter *et al.*, 1992; Ervasti and Campbell, 1993; Williams and Bloch, 1999) that is thought to mechanically stabilize the sarcolemmal membrane from shear stresses imposed during eccentric muscle contraction (Petrof *et al.*, 1993; Straub *et al.*, 1997). Biochemical studies have demonstrated that dystrophin contains two distinct and spatially separated actin binding sites located at the amino terminus and within the middle third of the large rod domain (Ryba-

kova *et al.*, 1996; Amann *et al.*, 1998). The two actin binding sites of dystrophin form an extended lateral contact with actin filaments and protect them from depolymerization *in vitro* (Rybakova *et al.*, 1996; Rybakova and Ervasti, 1997). More recently, we demonstrated that dystrophin is necessary for a mechanically strong physical link between the sarcolemma and actin filaments of costameres (Rybakova *et al.*, 2000).

Utrophin is a widely expressed autosomal gene product with high sequence similarity to dystrophin (Tinsley *et al.*, 1992). Utrophin is distributed throughout the sarcolemma in fetal and regenerating muscle, but is down-regulated in normal adult muscle and restricted to the myotendinous and neuromuscular junctions (Blake *et al.*, 1996). Because utrophin and dystrophin bind the same complement of proteins (Matsumura *et al.*, 1992; Kramarcy *et al.*, 1994; Winder *et al.*, 1995), it was hypothesized that utrophin may be capable of compensating for dystrophin deficiency. Indeed, transgenic overexpression of utrophin in dystrophin-deficient *mdx* mice resulted in full recovery for all known parameters of the dystrophic phenotype (Tinsley *et al.*, 1998). Based on these

Article published online ahead of print. Mol. Biol. Cell 10.1091/mbc.01-09-0446. Article and publication date are at [www.molbiolcell.org/cgi/doi/10.1091/mbc.01-09-0446](http://www.molbiolcell.org/cgi/doi/10.1091/mbc.01-09-0446).

§ Corresponding author. E-mail address: [ervasti@physiology.wisc.edu](mailto:ervasti@physiology.wisc.edu).

promising results, utrophin up-regulation or gene therapy is under intense investigation as a potential therapy for Duchenne muscular dystrophy. Recent results, however, have raised concern about whether utrophin can effect the same mechanically strong link with costameric actin as provided by dystrophin (Rybakova *et al.*, 2000). Although endogenous utrophin expression is up-regulated in striated muscle of *mdx* mice (Matsumura *et al.*, 1992; Porter *et al.*, 1998) and partially attenuates the phenotype associated with dystrophin deficiency (Deconinck *et al.*, 1997a; Grady *et al.*, 1997), this level of utrophin expression was not sufficient to retain costameric actin filaments on mechanically isolated sarcolemma (Rybakova *et al.*, 2000). In addition, sequence comparisons (Winder, 1997; Amann *et al.*, 1999) and biochemical analysis of recombinant protein fragments (Winder *et al.*, 1995; Amann *et al.*, 1998, 1999; Renley *et al.*, 1998; Moores and Kendrick-Jones, 2000) have indicated that dystrophin and utrophin may bind F-actin through distinct mechanisms. Most notably, utrophin lacks the actin binding region composed of basic spectrin-like repeats that is present in the middle rod domain of dystrophin (Amann *et al.*, 1999). These data suggested that utrophin may bind actin filaments solely through its amino-terminal calponin homology domain, and with an order of magnitude lower affinity (Winder *et al.*, 1995; Moores and Kendrick-Jones, 2000) compared with dystrophin (Rybakova *et al.*, 1996).

Herein, we have expressed full-length recombinant utrophin and show that the protein exhibits a native molecular weight and molecular dimensions indicative of a monomer. Contrary to expectations, full-length utrophin bound laterally along actin filaments with high affinity and protected filaments from depolymerization *in vitro*. Compared with dystrophin, utrophin made less extensive lateral contact with actin filaments and through distinct molecular epitopes. We also demonstrate that costameric actin is rescued on mechanically isolated sarcolemma from transgenic *mdx* mice that overexpress utrophin (Tinsley *et al.*, 1998). Our results indicate that utrophin can perform all the actin binding functions documented for dystrophin. These data strongly support the continued exploration of therapies aiming to treat Duchenne muscular dystrophy through interventions that increase utrophin expression.

## MATERIALS AND METHODS

### Recombinant Utrophin

The 11-kb *Bam*HI/*Xba*I fragment from a vector encoding full-length mouse utrophin with an amino-terminal FLAG epitope (Guo *et al.*, 1996) was ligated into the *Bam*HI/*Xba*I site of pFASTBAC1 donor plasmid. The recombinant plasmid was transformed into DH10BAC cells for site-specific transposition into bMON14272 bacmid DNA. High-titer viral stocks were used to infect  $5 \times 177$ -cm<sup>2</sup> Sf21 cell monolayers, which were harvested 72 h postinfection and resuspended in 10 ml of 50 mM Tris-HCl, pH 7.4, 150 mM NaCl, 1% Triton X-100, and a cocktail of protease inhibitors (Rybakova *et al.*, 1996). The lysate was circulated over a 2-ml anti-FLAG M2 agarose column (Sigma-Aldrich, St. Louis, MO), which was washed extensively with buffer A (10 mM Tris-HCl, pH 7.4, 150 mM NaCl, and 0.1% Triton X-100) and bound utrophin eluted with buffer A containing 100  $\mu$ g/ml FLAG peptide (Sigma-Aldrich). For protein used in rotary shadowing, the M2 column was washed and eluted as described above except that Triton X-100 was omitted. Purified utrophin was concentrated in a Centricon 100 (Amicon, Beverly,

MA) and assayed for protein with the Bio-Rad DC protein assay kit by using bovine serum albumin as standard. The typical yield of pure utrophin was 700  $\mu$ g from  $5 \times 177$  cm<sup>2</sup> of cell monolayer. Recombinant utrophin was analyzed on Coomassie blue-stained SDS-polyacrylamide gels and by Western blot analysis with the utrophin-specific monoclonal antibodies MANCHO3 (Man *et al.*, 1991) and DRP-2 (Novocastra, New Castle, UK), and with anti-FLAG clone M2 (Sigma-Aldrich).

### Recombinant Utrophin N-Terminal Actin Binding Domains

To generate an expression vector encoding mouse utrophin amino acids 1–261 fused with an amino-terminal FLAG epitope (FLAG-UTR261), the oligonucleotide primers 5'-TATTCCGGATTATTCA-TACC-3' and 5'-GCACCTCTCGAGTTCATCTAT-3' were used to polymerase chain reaction-amplify a cDNA encoding FLAG-UTR261 from the pFASTBAC1 donor plasmid containing full-length, FLAG-utrophin. The polymerase chain reaction product was subcloned into pCR-Blunt (Invitrogen, Carlsbad, CA), cut out with *Bam*HI and *Xho*I, and inserted between the *Bam*HI and *Xho*I sites of pET23 (Novagen, Madison, WI). Both FLAG-UTR261 and an untagged construct (UTR261+) were expressed in *Escherichia coli* strain BL21 (DE3) and purified by serial ion exchange and gel filtration chromatography essentially as described previously (Moores and Kendrick-Jones, 2000).

### Hydrodynamic Analysis

Measurement of the sedimentation coefficient and Stokes radius and calculation of the native molecular weight and frictional coefficient of recombinant utrophin were performed as described previously (Rybakova and Ervasti, 1997; Amann *et al.*, 1999).

### Electron Microscopy

Recombinant utrophin was diluted 10-fold into 0.15 M ammonium bicarbonate/acetate, pH 7.4, and adjusted to 55% glycerol. Low-angle rotary shadowing and electron microscopy were performed as described previously (Yurchenco and Cheng, 1993).

### Actin Binding Analysis

Recombinant utrophin binding to muscle and nonmuscle F-actin (Cytoskeleton, Denver, CO) was measured as described previously (Rybakova *et al.*, 1996). Briefly, purified recombinant utrophin or utrophin fragments were incubated with 6  $\mu$ M F-actin in actin binding buffer (10 mM Tris-HCl, pH 8.0, 0.1 mM ATP, 2 mM MgCl<sub>2</sub>, 0.2 mM dithiothreitol, and 0.1% Triton X-100) also containing 100 mM NaCl and centrifuged at  $100,000 \times g$  for 20 min. The resulting supernatants and F-actin pellets were resolved on Coomassie blue-stained SDS-polyacrylamide gels and the amount of bound and free protein measured by densitometry. The effect of utrophin on F-actin depolymerization was assessed by high-speed cosedimentation after dilution into low ionic strength buffer as described previously (Rybakova *et al.*, 1996; Rybakova and Ervasti, 1997). Briefly, various concentrations of utrophin were preincubated for 20 min with F-actin in actin binding buffer containing 30 mM NaCl and then diluted with actin binding buffer to final actin and NaCl concentrations of 2  $\mu$ M and 4.5 mM, respectively. At various times postdilution, samples were centrifuged and analyzed for the fraction of actin remaining in the pellet as described above.

### Analysis of Mechanically Peeled Sarcolemma and Myofibers

Sarcolemma and peeled myofibers were isolated from the extensor digitorum longus muscles of age-matched *mdx*, and Fiona transgenic *mdx* mice (Tinsley *et al.*, 1998) and visualized by confocal

microscopy as described previously (Rybakova *et al.*, 2000). F-actin was detected with Alexa568-phalloidin (Molecular Probes) and utrophin was stained with rabbit 56 antiserum (Rybakova *et al.*, 2000) or monoclonal antibody (mAb) DRP1 (Novocastra).

### Quantitation of Utrophin Protein Expression in Muscle

Trunk and limb muscles of C57BL/10ScSn control (Jackson Laboratories, Bar Harbor, ME), *mdx*, and Fiona transgenic *mdx* mice were snap frozen in liquid nitrogen, and stored at  $-80^{\circ}\text{C}$ . Frozen muscle (0.5 g) was pulverized in a mortar and pestle, cooled with liquid nitrogen, and solubilized in 2 ml of 1% SDS, 5 mM EGTA, and a cocktail of protease inhibitors. The samples were incubated for 2 min at  $100^{\circ}\text{C}$  and centrifuged at  $12,000 \times g$ . The protein concentration of the supernatants was measured with the Bio-Rad DC protein assay kit by using bovine serum albumin as standard. Nitrocellulose transfers containing various amounts of protein were incubated with a 1:200 dilution of mAb MANCHO3 (Man *et al.*, 1991) and immunoreactivity was detected with  $^{125}\text{I}$ -goat anti-mouse IgG and autoradiography. The intensities of immune signal were analyzed densitometrically. A standard curve of purified recombinant utrophin was included on all gels/transfers.

## RESULTS

### Expression, Purification, and Characterization of Recombinant Utrophin

The actin binding properties of utrophin have only been extrapolated from studies of small recombinant fragments (Winder *et al.*, 1995; Amann *et al.*, 1999; Moores and Kendrick-Jones, 2000; Zuellig *et al.*, 2000). Therefore, we generated a baculovirus construct encoding full-length mouse utrophin with an amino-terminal FLAG epitope (Figure 1A). Coomassie blue-stained gels of infected cell lysates (Figure 1B) revealed a novel protein with an average molecular weight of 379,000. The protein was confirmed as intact FLAG-tagged utrophin on Western blots stained with antibodies to either the amino or carboxyl termini of utrophin and by M2 antibody to the FLAG epitope (Figure 1, A and B). Both the anti-FLAG and utrophin amino-terminal, but not the carboxy-terminal antibodies also reacted with a second band of  $\sim 300,000$  molecular weight (Figure 1B), which was probably a proteolytic fragment. Recombinant utrophin was purified using anti-Flag M2 agarose chromatography (Figure 1C). Densitometry indicated that full-length utrophin comprised  $\sim 95\%$  of the recovered protein. The remaining  $\sim 5\%$  was due to the  $\sim 300,000$  molecular weight proteolytic fragment (Figure 1C). From the measured Stokes' radius (9.1 nm) and sedimentation coefficient (10.4 S), we calculated a native molecular weight of 404,000 for recombinant utrophin, which was within  $\sim 3\%$  of its predicted molecular weight of 393,000. The calculated frictional coefficient (1.86) suggested that purified recombinant utrophin assumed an asymmetric rod shape as predicted previously (Tinsley *et al.*, 1992).

Although dystrophin and utrophin are widely envisioned as highly flexible rod-shaped molecules, the experimental evidence in support of such a model is minimal (Pons *et al.*, 1990). Therefore, we examined recombinant utrophin by electron microscopy after rotary shadowing (Figure 2). The distribution of molecules was sparse due to the marginal solubility of utrophin in the buffer necessary for rotary shadowing. However, the observed molecules predominantly

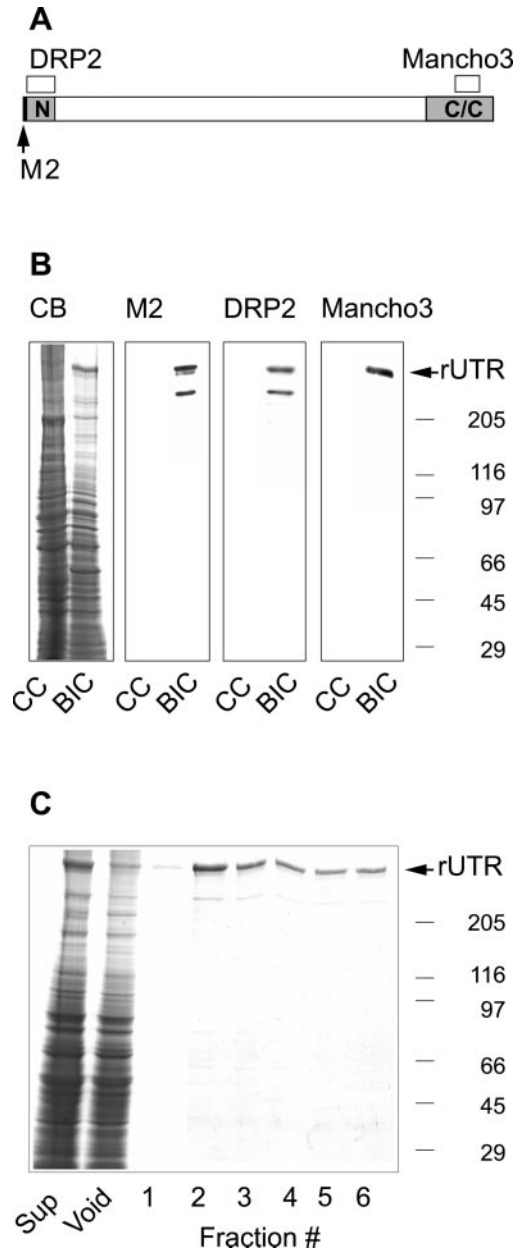


**Figure 1.** Expression and purification of recombinant utrophin. (A) Schematic of utrophin with the locations of epitopes for anti-FLAG M2, DRP2, and MANCHO3 monoclonal antibodies. (B) Coomassie blue-stained SDS-polyacrylamide gel (CB) and identical nitrocellulose transfers containing uninfected Sf21 cells (CC), and Sf21 cells infected with recombinant baculovirus encoding full-length utrophin (BIC). The arrow identifies the high molecular weight novel protein apparent in BIC stained with Coomassie blue and reactive with utrophin and anti-FLAG antibodies. (C) Coomassie blue-stained gel loaded with equivalent volumes of infected insect cell proteins solubilized with 1% Triton X-100 (Sup), the anti-FLAG M2 agarose void, and fractions eluted with FLAG peptide. The molecular weight standards ( $\times 10^{-3}$ ) are indicated on the right.

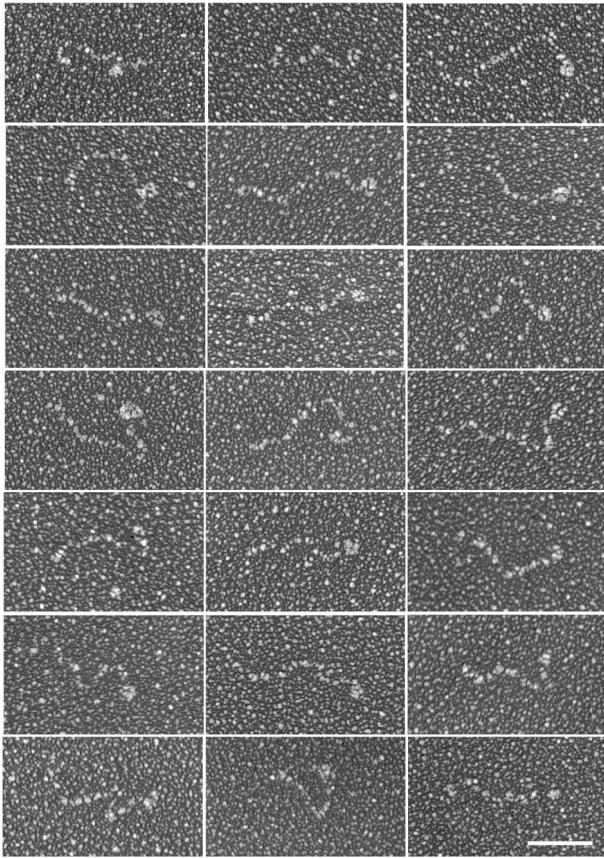


**Figure 2.** Rotary shadowed utrophin. Shown are images selected to display the array of molecular configurations observed. The average contour length was  $118 \pm 22$  nm ( $n = 59$ ) and most molecules exhibited a globular structure at one end. Bar, 50 nm.

appeared as highly elongated structures with an average contour length of  $118 \pm 22$  nm ( $\pm$  SD,  $n = 59$ ). Based on available molecular dimensions (Yan *et al.*, 1993; Keep *et al.*, 1999), the amino-terminal actin binding domain and 22 spectrin-like repeats of utrophin would be expected to span a length of 115 nm. The globular structure near one end of most molecules may represent the cysteine-rich and C-terminal domains of utrophin because these domains were absent from the proteolytic fragment in purified utrophin (Figure 1) and the cysteine-rich domain of dystrophin adopts a globular structure (Huang *et al.*, 2000). Finally, the molecules displayed random bends or kinks throughout their length, suggesting that utrophin is very flexible.

#### **Actin Binding Properties of Recombinant Utrophin**

High-speed cosedimentation analysis demonstrated that recombinant utrophin bound saturably to skeletal muscle F-actin with a  $K_d$  of  $0.15 \pm 0.06$   $\mu$ M and a  $B_{max}$  of 1 mol of utrophin/14 mol of actin, whereas virtually no utrophin sedimented in the absence of F-actin (Figure 3, A and B). Utrophin bound nonmuscle actin with a similar  $K_d$  of  $0.24 \pm 0.03$   $\mu$ M, indicating no marked preference for different actin

isoforms. A recombinant protein encoding utrophin amino acids 1–261 fused with an amino-terminal FLAG epitope (FLAG-UTR261) and an untagged construct (UTR261+) both bound F-actin with 1:1 stoichiometry and  $K_d$  values of  $16.5 \pm 5.1$  and  $7.1 \pm 4.1$   $\mu$ M, respectively. Thus, the FLAG epitope cannot account for the dramatic differences in actin binding properties between full-length utrophin and the isolated amino-terminal actin binding domain. Most interesting, the surprisingly high affinity and low stoichiometry of full-length utrophin binding to F-actin indicate that the rod domain also participates in utrophin binding to actin.

Because only two spectrin repeats in utrophin are basic, it seemed likely that the utrophin rod domain participates in actin binding through a nonelectrostatic mechanism. We found that utrophin binding to F-actin was insensitive to NaCl concentrations up to 0.8 M (Figure 3C). In contrast, dystrophin binding to F-actin was significantly inhibited by 0.5 M NaCl (Rybakova *et al.*, 1996). Utrophin would also be expected to significantly slow the depolymerization of actin filaments as shown previously for dystrophin (Rybakova *et al.*, 1996). As predicted, we found that F-actin depolymerization was significantly slowed in the presence of utrophin (Figure 4A). However, the protective effect of utrophin on actin depolymerization was more transient, lasting only 80 min compared with dystrophin, which persisted for at least 4 h (Rybakova *et al.*, 1996). The protective effect of utrophin on F-actin depolymerization saturated at a utrophin: actin molar ratio of 1 utrophin:14 actin monomers (Figure 4B), which is highly consistent with the stoichiometry measured at equilibrium. In total, our results suggest that utrophin binds with high affinity along side an actin filament and can stabilize F-actin *in vitro* in a manner analogous to dystrophin. However, the decreased stoichiometry of utrophin binding to F-actin and its insensitivity to increased ionic strength further suggests that utrophin binds laterally along actin filaments through molecular contacts that are distinct from those used by dystrophin.

#### **Utrophin Overexpression Rescues Costameric Actin Defect of mdx Muscle**

We recently demonstrated that a population of actin filaments colocalized with dystrophin in a costameric pattern on sarcolemma peeled from single myofibers of normal mouse muscle (Rybakova *et al.*, 2000). In contrast, costameric actin was uniformly absent from sarcolemma of dystrophin-deficient *mdx* muscle even though utrophin was markedly up-regulated and retained in a costameric pattern (Rybakova *et al.*, 2000). We have now peeled sarcolemma from myofibers of a transgenic *mdx* mouse line (Fiona) that overexpresses full-length utrophin to levels that correct all other phenotypic parameters associated with dystrophin deficiency (Tinsley *et al.*, 1998). Strikingly, 18 of 19 sarcolemma from two different Fiona mice displayed bright phalloidin staining in a well organized costameric pattern that closely overlapped with utrophin (Figure 5). The one Fiona sarcolemma without phalloidin staining also failed to exhibit any utrophin immunoreactivity. In contrast to the uniform retention of costameric actin on sarcolemma from the Fiona line, phalloidin staining was absent in nine of nine sarcolemma from two age-matched *mdx* mice, although costameric utrophin was present on all specimens (Figure 5). Thus, when overexpressed to sufficiently high levels, utro-

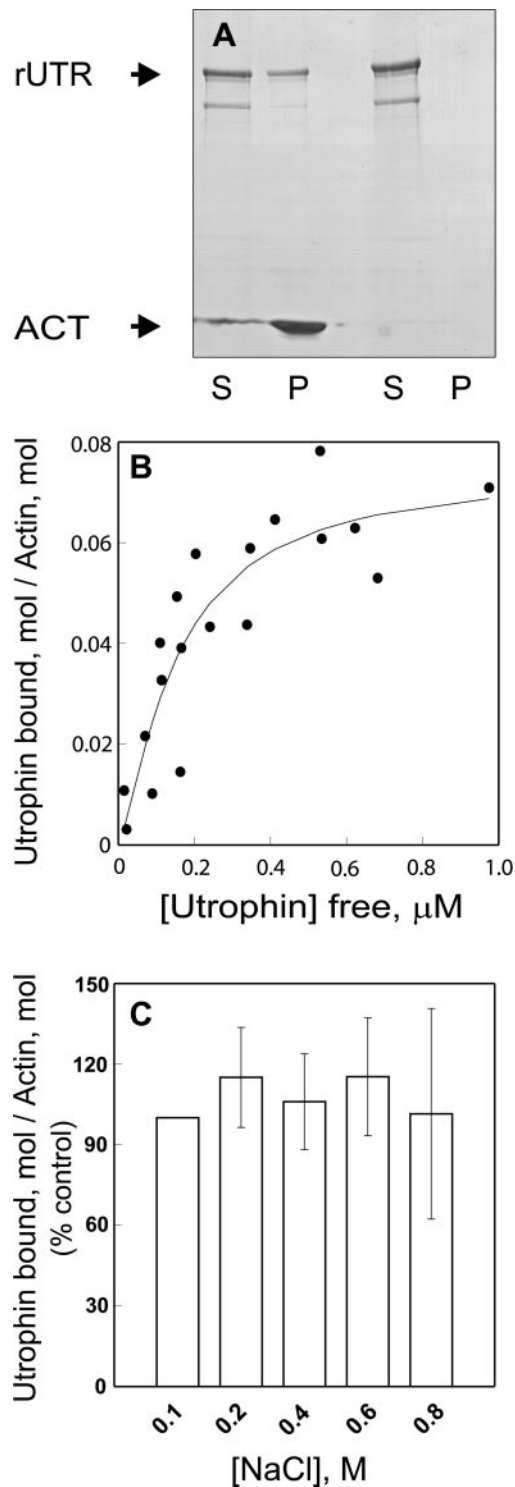


**Figure 3.** Utrophin binding to F-actin. (A) Coomassie blue-stained SDS-polyacrylamide gel of the supernatant (S) and pellet (P) recovered after  $0.6 \mu\text{M}$  recombinant utrophin (rUTR) was centrifuged at  $100,000 \times g$  in the presence or absence of  $6 \mu\text{M}$  skeletal muscle F-actin (ACT). (B) Increasing concentrations of recombinant utrophin were incubated with  $6 \mu\text{M}$  F-actin with subsequent centrifugation. The amount of free and actin-bound utrophin was deter-

mined densitometrically from Coomassie blue-stained gels of supernatant and pellet fractions. Symbols represent data from two independent experiments performed with different utrophin preparations. Nonlinear regression analysis yielded a  $K_d$  value of  $0.2 \mu\text{M}$  and a  $B_{\text{max}}$  value of 1 utrophin:14 actin monomers. (C) Utrophin ( $0.2 \mu\text{M}$ ) was incubated with  $6 \mu\text{M}$  F-actin over a range of NaCl concentrations ( $0.1$ – $0.8 \text{ M}$ ) and subjected to centrifugation at  $100,000 \times g$ . The binding data ( $n = 3$ ) were normalized against the amount of actin pelleted and expressed as the percentage of utrophin cosedimented with F-actin in  $0.1 \text{ M}$  NaCl.

### Quantitation of Utrophin Expression in Control, *mdx*, and Fiona Mice

Based on our results, utrophin can perform all of the in vitro and in vivo actin binding functions previously documented for dystrophin. However, it remained unclear how much utrophin is required to correct the *mdx* phenotype relative to the amount of dystrophin normally expressed in wild-type muscle. Therefore, we measured utrophin abundance in skeletal muscle of control, *mdx*, and Fiona mice by quantitative Western blot analysis with recombinant utrophin as a standard (Figure 6). Both the 43-kDa actin-containing band and the 205-kDa myosin heavy chain band exhibited nearly identical densitometric intensities on Coomassie blue-stained gels when equal amounts of total protein were loaded for control, *mdx*, and Fiona muscle (Figure 6A). Furthermore, Western blots loaded with equal amounts of total muscle protein for each mouse line yielded nearly identical autoradiographic intensities when stained with a mAb specific for  $\alpha$ -sarcomeric actin and detected with  $^{125}\text{I}$ -goat anti-mouse secondary (Figure 6A). For utrophin, however, we found it necessary to load different amounts of protein from the three mouse lines to ensure that immune signals from each were measured in the linear range (Figure 6B). Control muscle exhibited the lowest utrophin abundance ( $0.00058 \pm 0.00053\%$ ), whereas the highest utrophin level was measured in Fiona muscle ( $0.014 \pm 0.0015\%$ ). In good agreement with previous measurements of relative abundance (Matsumura *et al.*, 1992; Porter *et al.*, 1998), the utrophin content of *mdx* muscle ( $0.0013 \pm 0.00014\%$ ) was approximately two-fold greater than that of control muscle. Interestingly, the absolute utrophin abundance of *mdx* muscle was  $>60\%$  of a previous estimate of dystrophin abundance in control muscle (Hoffman *et al.*, 1987). Because the bulk of utrophin immunoreactivity in normal skeletal muscle cross sections is localized to nonmuscle cell types (Rivier *et al.*, 1997; Peters *et al.*, 1998), it could be argued that utrophin abundance in *mdx* muscle should be corrected by subtracting the amount of utrophin expressed in normal muscle ( $0.00058\%$ ). Even with this correction, however, our results suggest that the utrophin content of *mdx* muscle ( $0.00072\%$ ) approaches one-third of the measured dystrophin abundance ( $0.002\%$ ) in normal muscle (Hoffman *et al.*, 1987).

### DISCUSSION

Studies in knock-out and transgenic mice have provided compelling evidence that utrophin can compensate for many

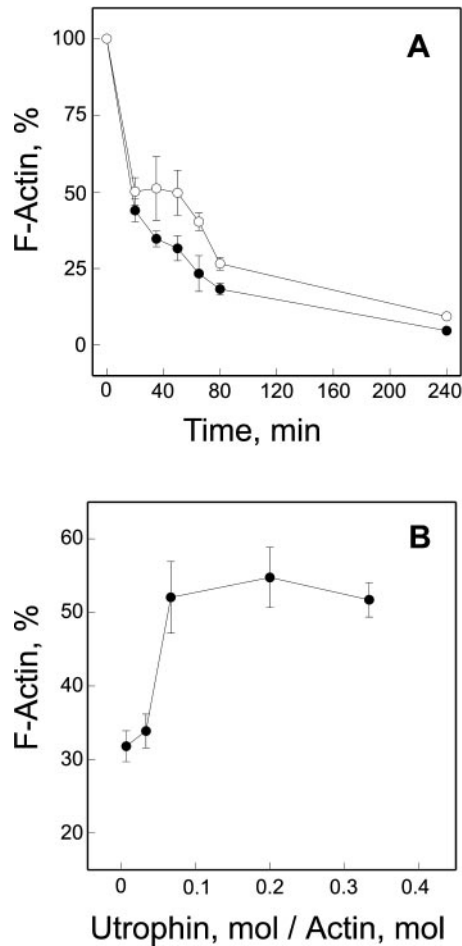


**Figure 4.** Effect of utrophin on F-actin depolymerization. (A) Time course of actin depolymerization in the absence (●) or presence of utrophin (○). F-actin was preincubated alone or in a 10:1 M ratio with utrophin and filament depolymerization was induced by dilution to final actin and NaCl concentrations of 2  $\mu$ M and 4.5 mM, respectively. At various times postdilution, samples were centrifuged at  $100,000 \times g$  for 20 min and the fraction of F-actin remaining was determined densitometrically from Coomassie blue-stained gels loaded with equal volumes of supernatants and pellets. Time points include centrifugation time. (B) F-actin was preincubated with increasing amounts of utrophin to give the indicated utrophin/actin monomer ratio and depolymerization was initiated by dilution as described above. Thirty minutes after initiation of depolymerization, samples were centrifuged at  $100,000 \times g$  and the percentage of F-actin remaining was determined as in A. The data represent the average ( $\pm$  SEM) from five (A) and three (B) independent experiments.

of the functions normally performed by dystrophin in skeletal muscle (Tinsley *et al.*, 1996, 1998; Deconinck *et al.*, 1997a, b; Grady *et al.*, 1997). Herein, we have demonstrated that utrophin can retain costameric actin on mechanically peeled sarcolemma when overexpressed in *mdx* muscle to levels that also correct all other known parameters of the *mdx* phenotype. These results simultaneously validate the costameric actin defect of *mdx* sarcolemma (Rybakova *et al.*, 2000) as a direct consequence of dystrophin deficiency and

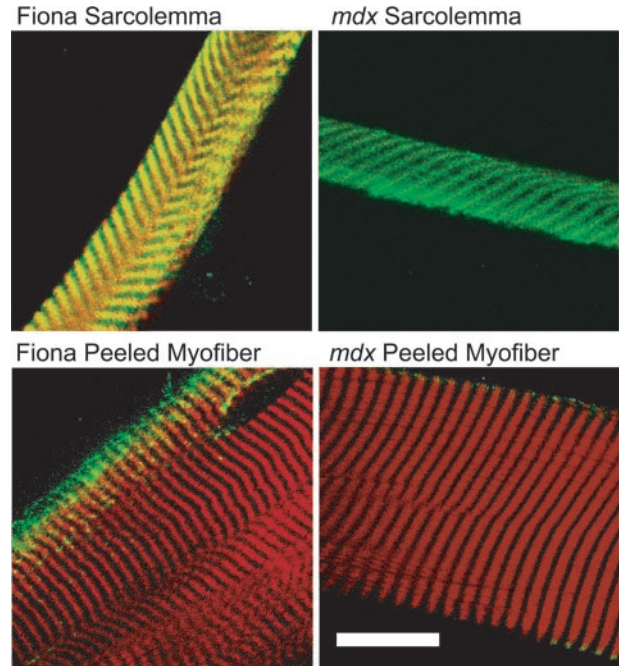


**Figure 5.** Utrophin overexpression in *mdx* mice rescues costameric actin on mechanically peeled sarcolemma. Shown are images of mechanically peeled sarcolemma, or myofibers stained with Alexa568-phalloidin (red) and rabbit 56 antiserum to utrophin (green), with areas of coincidence appearing yellow. Specimens were obtained from transgenic *mdx* mice overexpressing utrophin (Fiona), or from age-matched *mdx* mice. Bar, 20  $\mu$ m.

reinforce the hypothesis that utrophin and dystrophin are functionally interchangeable.

Given the differences between analogous domains in primary structure (Winder, 1997; Amann *et al.*, 1999) and actin binding properties (Winder *et al.*, 1995; Amann *et al.*, 1998, 1999; Renley *et al.*, 1998; Moores and Kendrick-Jones, 2000), it was expected that utrophin would bind actin filaments through a mechanism distinct from the lateral attachment used by dystrophin. Surprisingly, we have demonstrated that recombinant utrophin bound actin filaments with significantly higher affinity and through a more extensive lateral association than was anticipated. Our experiments indicate that full-length utrophin can occupy 14 actin monomers when saturating an actin filament compared with the one-to-one association consistently observed with the isolated utrophin amino-terminal actin binding domain (Moores and Kendrick-Jones, 2000). Our previous studies (Rybakova *et al.*, 1996; Rybakova and Ervasti, 1997; Amann *et al.*, 1999) indicated that 17 spectrin repeats allow dystrophin to associate with 24 monomers in an actin filament (Figure 7). Assuming that a similar repeat/actin monomer ratio holds for utrophin, our data predict that perhaps the first 10 spectrin-like repeats participate in the actin binding activity of utrophin (Figure 7). Interestingly, a recombinant protein corresponding to the amino-terminal actin binding domain and first 2.5 spectrin-like repeats of utrophin (Zuelig *et al.*, 2000) bound F-actin with an affinity (2  $\mu$ M) and stoichiometry (1:5) intermediate to that observed for the

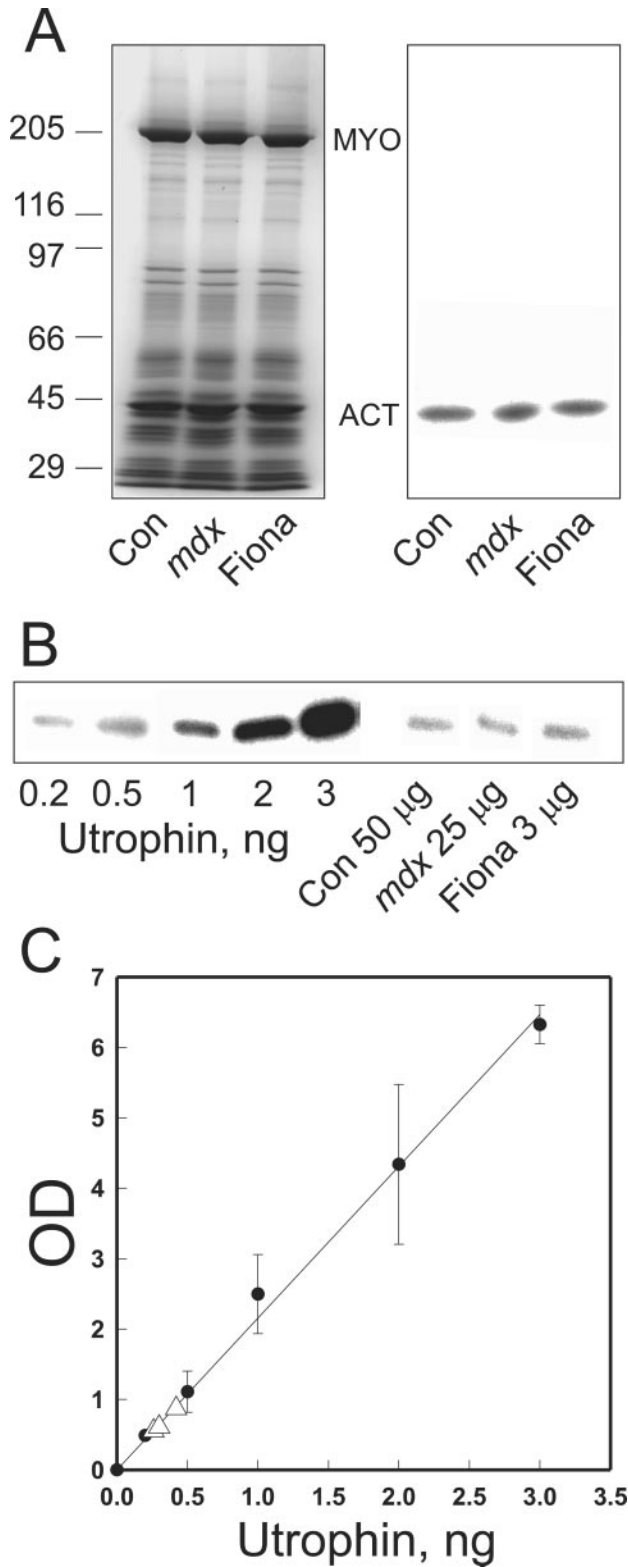


**Figure 6.** Utrophin protein abundance in control, *mdx*, and Fiona transgenic *mdx* mice. (A) Coomassie blue-stained gel (left) or nitrocellulose transfer (right) loaded with equal amounts of total protein

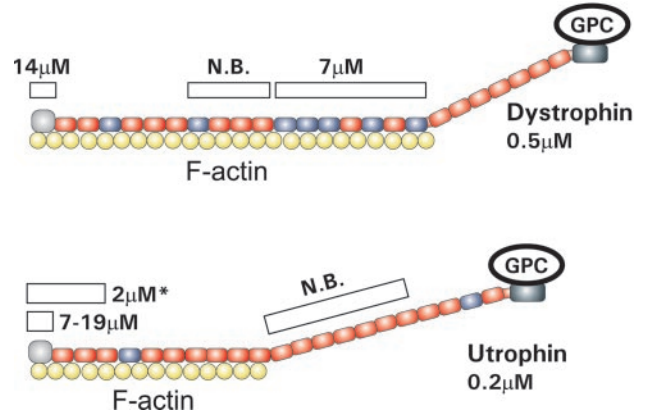


**Figure 7.** Side binding model for dystrophin and utrophin binding to actin filaments. Shown are schematic diagrams of dystrophin and utrophin complexed with F-actin. Red spectrin-like repeats are acidic, and blue repeats are basic. The white bars above dystrophin and utrophin represent the recombinant fragments for each protein that have been analyzed for actin binding activity with the measured affinities indicated. N.B., no binding observed. The fragment marked with an asterisk was described in Zuellig *et al.* (2000).

N-terminal actin binding domain alone (7–19 µM, 1:1) and full-length utrophin (0.2 µM, 1:14). Although we are not aware of any studies that have explicitly tested whether the C-terminal region of utrophin binds to F-actin, the homologous region of dystrophin failed to bind F-actin as assessed by high-speed cosedimentation (Corrado *et al.*, 1994). Moreover, we previously detected no F-actin cosedimentation by the C-terminal dystrophin fragment or dystrophin associated proteins after calpain digestion of purified dystrophin-glycoprotein complex (Rybakova *et al.*, 1996). Finally, dystrophin and utrophin would be expected to bind actin filaments with similar stoichiometries if they bound filaments through N- and C-terminal binding sites. However, our data indicate that utrophin interacts with fewer actin monomers in filaments compared with dystrophin. Based on current data, we propose that the actin binding region of utrophin spans from its amino terminus through repeat 10, whereas that of dystrophin extends out through repeat 17 (Figure 7). The participation of 10 spectrin-like repeats in utrophin binding to F-actin may explain why a utrophin construct lacking repeats 4–19 was less effective than full-length utrophin in ameliorating the phenotypes associated with dystrophin deficiency in *mdx* mice (Deconinck *et al.*, 1997b; Tinsley *et al.*, 1998).

from control, *mdx*, and Fiona muscle. The transfer was stained with a mAb specific for  $\alpha$ -sarcomeric actin detected with  $^{125}\text{I}$ -anti-mouse IgG. Molecular weight standards ( $\times 10^{-3}$ ) are shown on the left. (B) Autoradiogram from a nitrocellulose transfer containing the various amounts of purified utrophin, 50 µg of control, 25 µg of *mdx*, and 3 µg of Fiona total skeletal muscle extract stained with MANCHO3 and detected by  $^{125}\text{I}$ -anti-mouse IgG. (C) Standard curve of autoradiographic intensity vs. utrophin load from the autoradiogram in B. The utrophin signals obtained for muscle from the three lines of mice are indicated by open triangles. The utrophin content of control, *mdx*, and Fiona muscle was  $0.00058 \pm 0.000053$ ,  $0.0013 \pm 0.00014$ , and  $0.014 \pm 0.0015\%$ , respectively (n = 4).

Because the utrophin rod domain lacks a cluster of basic, spectrin-like repeats (Amann *et al.*, 1999), it is likely that utrophin repeats interact with actin filaments through a molecular mechanism that is distinct from the electrostatic interaction used by the dystrophin middle rod domain (Amann *et al.*, 1998). Indeed, we observed that utrophin binding to F-actin was insensitive to NaCl concentrations (Figure 4) that significantly inhibited dystrophin binding to F-actin (Rybakova *et al.*, 1996). A contribution by the spectrin-like repeats most proximal to the N-terminal actin binding activity of utrophin and dystrophin may explain why dystrophin constructs containing only five spectrin-like repeats can rescue the *mdx* phenotype (Wang *et al.*, 2000), whereas constructs lacking the entire rod domain failed to provide functional correction (Hartigan-O'Connor and Chamberlain, 2000). Our results further imply that the actin side binding function now demonstrated for vertebrate dystrophin and utrophin may be more widely conserved across invertebrate dystrophin family members than could be predicted by sequence comparisons (Greener and Roberts, 2000; Neuman *et al.*, 2001). More generally, we speculate that the combined presence of a CH-type actin binding domain and spectrin-like repeats may enable some members of the plakin family of cytolinkers to laterally bind and stabilize actin filaments (Leung *et al.*, 2001). In support of this possibility, actin filaments associated with microtubule-bound microtubule actin crosslinking factor (MACF) were recently found to be more resistant to depolymerization induced by latrunculin B (Karakesisoglou *et al.*, 2000).

We have also made use of purified recombinant utrophin as a standard to estimate the absolute utrophin protein content in control, *mdx*, and the Fiona line of transgenic mice. The utrophin content of Fiona muscle was ~10-fold greater than that of *mdx* muscle and also approximately sevenfold greater than the dystrophin content of control muscle (Hoffman *et al.*, 1987). A 50-fold overexpression of dystrophin was previously shown to correct the *mdx* phenotype without any toxic side effects (Cox *et al.*, 1993). At present, it is not possible to determine the minimal level of utrophin expression necessary for retention of costameric actin on isolated sarcolemma, or for full correction of the dystrophic phenotype. However, utrophin expression in *mdx* muscle was greater than 60% of a similarly determined estimate of dystrophin content in striated muscle from normal mice (Hoffman *et al.*, 1987). Even after correction for nonmuscle utrophin expression, our current measurements indicate that *mdx* muscle up-regulates utrophin expression to 36% of dystrophin levels in normal muscle, which may explain its milder phenotype compared with mice deficient in both dystrophin and utrophin (Deconinck *et al.*, 1997a; Grady *et al.*, 1997). On the other hand, transgenic expression of dystrophin to 20% of its normal levels was sufficient to prevent essentially all dystrophic symptoms in the *mdx* mouse (Phelps *et al.*, 1995). Thus, the presence of even mild phenotype despite significant levels of utrophin in *mdx* muscle can be interpreted several ways. First, the increased utrophin expression of *mdx* muscle may be preferentially concentrated within regenerating fibers although weak sarcolemmal utrophin staining is sometimes apparent in large diameter *mdx* muscle fibers with peripheral nuclei (Peters *et al.*, 1997). It is also possible that utrophin is less efficient in coupling the sarcolemma to costameres. Based on our depo-

lymerization experiments, utrophin/F-actin complexes may be kinetically less stable compared with dystrophin/F-actin complexes (Rybakova *et al.*, 1996), whereas other results (Lumeng *et al.*, 1999; Imamura *et al.*, 2000) suggest that the utrophin/ $\beta$ -dystroglycan interaction may be weaker. Alternatively, correction of the *mdx* phenotype by transgenic dystrophin expression to 20% of wild-type levels (Phelps *et al.*, 1995) may instead have been due to functional additivity with concomitant up-regulation of utrophin. Likewise, rescue of the *mdx* phenotype by truncated dystrophins (Wang *et al.*, 2000) may be due in part to additivity with the high utrophin levels endogenous to *mdx* muscle. Functional additivity further suggests that even low-level dystrophin expression induced by gene therapy when combined with pharmacological up-regulation of endogenous utrophin expression may yield an additive therapeutic benefit in patients with dystrophinopathies.

Due mainly to its exceedingly low abundance in native tissues, the biochemical characterization of utrophin function has previously relied on analysis of recombinant protein fragments (Winder *et al.*, 1995; Amann *et al.*, 1999; Chung and Campanelli, 1999; James *et al.*, 2000). Our actin binding studies of full-length recombinant utrophin suggest that the sum of the parts does not necessarily equal, or even accurately reflect the behavior of the whole. Future experiments will revisit models for the interaction between utrophin/dystrophin and  $\beta$ -dystroglycan, which currently rely almost exclusively on results with isolated protein fragments (Chung and Campanelli, 1999; Huang *et al.*, 2000; James *et al.*, 2000). Full-length recombinant utrophin will also be an invaluable probe to identify novel molecular partners. Finally, the utrophin prepared by these methods now make possible studies to characterize its mechanical properties at the level of single molecules (Rief *et al.*, 1999).

## ACKNOWLEDGMENTS

We are grateful to Drs. Ruslan Grishanin, Vadim Klenchin, and Paul Friesen for advice with the baculovirus expression system, and to Sarah Squire for technical assistance. We thank Drs. Kevin Campbell for rabbit 56 antiserum, Glenn Morris for MANCHO3 antibodies, and Steve Winder for the UTR261+ expression construct. This study was supported by National Institutes of Health grants AR42423 and AR01985 (to J.M.E.), the Muscular Dystrophy Association (to I.N.R.), and the Medical Research Council, United Kingdom (to K.E.D.).

## REFERENCES

- Amann, K.J., Guo, W.X.A., and Ervasti, J.M. (1999). Utrophin lacks the rod domain actin binding activity of dystrophin. *J. Biol. Chem.* 274, 35375–35380.
- Amann, K.J., Renley, B.A., and Ervasti, J.M. (1998). A cluster of basic repeats in the dystrophin rod domain binds F-actin through an electrostatic interaction. *J. Biol. Chem.* 273, 28419–28423.
- Blake, D.J., Tinsley, J.M., and Davies, K.E. (1996). Utrophin: a structural and functional comparison to dystrophin. *Brain Pathol.* 6, 37–47.
- Chung, W., and Campanelli, J.T. (1999). WW and EF hand domains of dystrophin-family proteins mediate dystroglycan binding. *Mol. Cell. Biol. Res. Commun.* 2, 162–171.



- Corrado, K., Mills, P.L., and Chamberlain, J.S. (1994). Deletion analysis of the dystrophin-actin binding domain. *FEBS Lett.* *344*, 255–260.
- Cox, G.A., Cole, N.M., Matsumura, K., Phelps, S.F., Hauschka, S.D., Campbell, K.P., Faulkner, J.A., and Chamberlain, J.S. (1993). Overexpression of dystrophin in transgenic *mdx* mice eliminates dystrophic symptoms without toxicity. *Nature* *364*, 725–729.
- Craig, S.W., and Pardo, J.V. (1983). Gamma actin, spectrin, and intermediate filament proteins colocalize with vinculin at costameres, myofibril-to-sarcolemma attachment sites. *Cell Motil.* *3*, 449–462.
- Deconinck, A.E., Rafael, J.A., Skinner, J.A., Brown, S.C., Potter, A.C., Metzinger, L., Watt, D.J., Dickson, J.G., Tinsley, J.M., and Davies, K.E. (1997a). Utrophin-dystrophin-deficient mice as a model for Duchenne muscular dystrophy. *Cell* *90*, 717–727.
- Deconinck, N., Tinsley, J., De Backer, F., Fisher, R., Kahn, D., Phelps, S., Davies, K., and Gillis, J.M. (1997b). Expression of truncated utrophin leads to major functional improvements in dystrophin-deficient muscles of mice. *Nat. Med.* *3*, 1216–1221.
- Ervasti, J.M., and Campbell, K.P. (1991). Membrane organization of the dystrophin-glycoprotein complex. *Cell* *66*, 1121–1131.
- Ervasti, J.M., and Campbell, K.P. (1993). A role for the dystrophin-glycoprotein complex as a transmembrane linker between laminin and actin. *J. Cell Biol.* *122*, 809–823.
- Ervasti, J.M., Ohlendieck, K., Kahl, S.D., Gaver, M.G., and Campbell, K.P. (1990). Deficiency of a glycoprotein component of the dystrophin complex in dystrophic muscle. *Nature* *345*, 315–319.
- Grady, R.M., Teng, H.B., Nichol, M.C., Cunningham, J.C., Wilkinson, R.S., and Sanes, J.R. (1997). Skeletal and cardiac myopathies in mice lacking utrophin and dystrophin: a model for Duchenne muscular dystrophy. *Cell* *90*, 729–738.
- Greener, M.J., and Roberts, R.G. (2000). Conservation of components of the dystrophin complex in *Drosophila*. *FEBS Lett.* *482*, 13–18.
- Guo, W.X.A., Nichol, M., and Merlie, J.P. (1996). Cloning and expression of full length mouse utrophin: the differential association of utrophin and dystrophin with AChR clusters. *FEBS Lett.* *398*, 259–264.
- Hartigan-O'Connor, D., and Chamberlain, J.S. (2000). Developments in gene therapy for muscular dystrophy. *Microsc. Res. Tech.* *48*, 223–238.
- Hoffman, E.P., Brown, R.H., and Kunkel, L.M. (1987). Dystrophin: the protein product of the Duchenne muscular dystrophy locus. *Cell* *51*, 919–928.
- Huang, X., Poy, F., Zhang, R., Joachimiak, A., Sudol, M., and Eck, M.J. (2000). Structure of a WW domain containing fragment of dystrophin in complex with  $\beta$ -dystroglycan. *Nat. Struct. Biol.* *7*, 634–638.
- Imamura, M., Araishi, K., Noguchi, S., and Ozawa, E. (2000). A sarcoglycan-dystroglycan complex anchors Dp116 and utrophin in the peripheral nervous system. *Hum. Mol. Genet.* *9*, 3091–3100.
- James, M., Nuttall, A., Ilesley, J.L., Ottersbach, K., Tinsley, J.M., and Winder, S.J. (2000). Adhesion-dependent tyrosine phosphorylation of  $\beta$ -dystroglycan regulates its interaction with utrophin. *J. Cell Sci.* *113*, 1717–1726.
- Karakisoglou, I., Yang, Y., and Fuchs, E. (2000). An epidermal plakin that integrates actin and microtubule networks at cellular junctions. *J. Cell Biol.* *149*, 195–208.
- Keep, N.H., Winder, S.J., Moores, C.A., Walke, S., Norwood, F.L.M., and Kendrick-Jones, J. (1999). Crystal structure of the actin-binding region of utrophin reveals a head-to-tail dimer. *Structure* *7*, 1539–1546.
- Kramarcy, N.R., Vidal, A., Froehner, S.C., and Sealock, R. (1994). Association of utrophin and multiple dystrophin short forms with the mammalian  $M_r$  58,000 dystrophin-associated protein (syntrophin). *J. Biol. Chem.* *269*, 2870–2876.
- Leung, C.A., Liem, R.K.H., Parry, D.A.D., and Green, K.J. (2001). The plakin family. *J. Cell Sci.* *114*, 3409–3410.
- Lumeng, C.N., Phelps, S.F., Rafael, J.A., Cox, G.A., Hutchinson, T.L., Begy, C.R., Adkins, E., Wiltshire, R., and Chamberlain, J.S. (1999). Characterization of dystrophin and utrophin diversity in the mouse. *Hum. Mol. Genet.* *8*, 593–599.
- Man, N., Ellis, J.M., Love, D.R., Davies, K.E., Gatter, K.C., Dickson, G., and Morris, G.E. (1991). Localization of the DMDL gene-encoded dystrophin-related protein using a panel of nineteen monoclonal antibodies: presence at neuromuscular junctions, in the sarcolemma of dystrophic skeletal muscle, in vascular and other smooth muscles, and in proliferating cell lines. *J. Cell Biol.* *115*, 1695–1700.
- Matsumura, K., Ervasti, J.M., Ohlendieck, K., Kahl, S.D., and Campbell, K.P. (1992). Association of dystrophin-related protein with dystrophin-associated proteins in *mdx* mouse muscle. *Nature* *360*, 588–591.
- Moores, C.A., and Kendrick-Jones, J. (2000). Biochemical characterization of the actin-binding properties of utrophin. *Cell Motil. Cytoskeleton* *46*, 116–128.
- Neuman, S., Kaban, A., Volk, T., Yaffe, D., and Nudel, U. (2001). The dystrophin/utrophin homologues in *Drosophila* and in sea urchin. *Gene* *263*, 17–29.
- Pardo, J.V., D'Angelo Siliciano, J., and Craig, S.W. (1983). A vinculin-containing cortical lattice in skeletal muscle: transverse lattice elements ("costameres") mark sites of attachment between myofibrils and sarcolemma. *Proc. Natl. Acad. Sci. USA* *80*, 1008–1012.
- Peters, M.F., Adams, M.E., and Froehner, S.C. (1997). Differential association of syntrophin pairs with the dystrophin complex. *J. Cell Biol.* *138*, 81–93.
- Peters, M.F., Sadoulet-Puccio, H.M., Grady, R.M., Kramarcy, N.R., Kunkel, L.M., Sanes, J.R., Sealock, R., and Froehner, S.C. (1998). Differential membrane localization and intermolecular associations of  $\alpha$ -dystrobrevin isoforms in skeletal muscle. *J. Cell Biol.* *142*, 1269–1278.
- Petrof, B.J., Shrager, J.B., Stedman, H.H., Kelly, A.M., and Sweeney, H.L. (1993). Dystrophin protects the sarcolemma from stresses developed during muscle contraction. *Proc. Natl. Acad. Sci. USA* *90*, 3710–3714.
- Phelps, S.F., Hauser, M.A., Cole, N.M., Rafael, J.A., Hinkle, R.T., Faulkner, J.A., and Chamberlain, J.S. (1995). Expression of full-length and truncated dystrophin mini-genes in transgenic *mdx* mice. *Hum. Mol. Genet.* *4*, 1251–1258.
- Pons, F., Augier, N., Heilig, R., Leger, J., Mornet, D., and Leger, J.J. (1990). Isolated dystrophin molecules as seen by electron microscopy. *Proc. Natl. Acad. Sci. USA* *87*, 7851–7855.
- Porter, G.A., Dmytrenko, G.M., Winkelmann, J.C., and Bloch, R.J. (1992). Dystrophin colocalizes with  $\beta$ -spectrin in distinct subsarcolemmal domains in mammalian skeletal muscle. *J. Cell Biol.* *117*, 997–1005.
- Porter, J.D., Rafael, J.A., Ragusa, R.J., Brueckner, J.K., Trickett, J.I., and Davies, K.E. (1998). The sparing of extraocular muscle in dystrophinopathy is lost in mice lacking utrophin and dystrophin. *J. Cell Sci.* *111*, 1801–1811.
- Renley, B.A., Rybakova, I.N., Amann, K.J., and Ervasti, J.M. (1998). Dystrophin binding to nonmuscle actin. *Cell Motil. Cytoskeleton* *41*, 264–270.

- Rief, M., Pascual, J., Saraste, M., and Gaub, H.E. (1999). Single molecule force spectroscopy of spectrin repeats: low unfolding forces in helix bundles. *J. Mol. Biol.* *286*, 553–561.
- Rivier, F., Robert, A., Hugon, G., and Mornet, D. (1997). Different utrophin and dystrophin properties related to their vascular smooth muscle distributions. *FEBS Lett.* *408*, 94–98.
- Rybakova, I.N., Amann, K.J., and Ervasti, J.M. (1996). A new model for the interaction of dystrophin with F-actin. *J. Cell Biol.* *135*, 661–672.
- Rybakova, I.N., and Ervasti, J.M. (1997). Dystrophin-glycoprotein complex is monomeric and stabilizes actin filaments in vitro through a lateral association. *J. Biol. Chem.* *272*, 28771–28778.
- Rybakova, I.N., Patel, J.R., and Ervasti, J.M. (2000). The dystrophin complex forms a mechanically strong link between the sarcolemma and costameric actin. *J. Cell Biol.* *150*, 1209–1214.
- Straub, V., Rafael, J.A., Chamberlain, J.S., and Campbell, K.P. (1997). Animal models for muscular dystrophy show different patterns of sarcolemmal disruption. *J. Cell Biol.* *139*, 375–385.
- Tinsley, J.M., Blake, D.J., Roche, A., Byth, B.C., Knight, A.E., Kendrick-Jones, J., Suthers, G.K., Love, D.R., Edwards, Y.H., and Davies, K.E. (1992). Primary structure of dystrophin-related protein. *Nature* *360*, 591–593.
- Tinsley, J., Deconinck, N., Fisher, R., Kahn, D., Phelps, S., Gillis, J.M., and Davies, K. (1998). Expression of full-length utrophin prevents muscular dystrophy in *mdx* mice. *Nat. Med.* *4*, 1441–1444.
- Tinsley, J.M., Potter, A.C., Phelps, S.R., Fisher, R., Trickett, J.I., and Davies, K.E. (1996). Amelioration of the dystrophic phenotype of *mdx* mice using a truncated utrophin transgene. *Nature* *384*, 349–353.
- Wang, B., Li, J., and Xiao, X. (2000). Adeno-associated virus vector carrying human mindystrophin genes effectively ameliorates muscular dystrophy in *mdx* mouse model. *Proc. Natl. Acad. Sci. USA* *97*, 13714–13719.
- Williams, M.W., and Bloch, R.J. (1999). Extensive but coordinated reorganization of the membrane skeleton in myofibers of dystrophic (*mdx*) mice. *J. Cell Biol.* *144*, 1259–1270.
- Winder, S.J. (1997). The membrane-cytoskeleton interface: the role of dystrophin and utrophin. *J. Muscle Res. Cell Motility* *18*, 617–629.
- Winder, S.J., Hemmings, L., Maciver, S.K., Bolton, S.J., Tinsley, J.M., Davies, K.E., Critchley, D.R., and Kendrick-Jones, J. (1995). Utrophin actin binding domain: analysis of actin binding and cellular targeting. *J. Cell Sci.* *108*, 63–71.
- Yan, Y., Winograd, E., Viel, A., Cronin, T., Harrison, S.C., and Branton, D. (1993). Crystal structure of the repetitive segments of spectrin. *Science* *262*, 2027–2030.
- Yurchenco, P.D., and Cheng, Y.-S. (1993). Self-assembly and calcium-binding sites in laminin. A three-arm interaction model. *J. Biol. Chem.* *268*, 17286–17299.
- Zuellig, R.A., Bornhauser, B.C., Knuesel, I., Heller, F., Fritschy, J.-M., and Schaub, M.C. (2000). Identification and characterization of transcript and protein of a new short N-terminal utrophin isoform. *J. Cell. Biochem.* *77*, 418–431.